creative commons

COMMONS DEED

저작자표시-비영리-변경금지 2.0 대한민국

이용자는 아래의 조건을 따르는 경우에 한하여 자유롭게

- 이 저작물을 복제, 배포, 전송, 전시, 공연 및 방송할 수 있습니다.

다음과 같은 조건을 따라야 합니다:

저작자표시. 귀하는 원저작자를 표시하여야 합니다.

비영리. 귀하는 이 저작물을 영리 목적으로 이용할 수 없습니다.

변경금지. 귀하는 이 저작물을 개작, 변형 또는 가공할 수 없습니다.

- 귀하는, 이 저작물의 재이용이나 배포의 경우, 이 저작물에 적용된 이용허락조건을 명확하게 나타내어야 합니다.
- 저작권자로부터 별도의 허가를 받으면 이러한 조건들은 적용되지 않습니다.

저작권법에 따른 이용자의 권리는 위의 내용에 의하여 영향을 받지 않습니다.

이것은 이용허락규약(Legal Code)을 이해하기 쉽게 요약한 것입니다.

Disclaimer

dCollection

공학석사학위논문

Reservoir Characterization Using Distance Based Ensemble Smoother with Permeability Distribution Pattern

유체투과율 분포패턴 거리기반의 앙상블 스무더를 이용한 저류층 특성화

2016 년 8 월

서울대학교대학원
에너지시스템공학부
이지윤

Abstract

A distance is the degree of model dissimilarity and it is important for effective model selection. This paper suggests a cross spatial pattern to find permeability distribution from an injector to a producer. The distance is defined as one minus correlation coefficient of permeability data obtained by the spatial pattern.

Using multi−dimensional scaling, initial 400 reservoir models are projected on two dimensions based on the distance. By K−medoids clustering, they are classified into 10 groups. One representative medoid is chosen with the least difference in productions from the reference field. Then, 100 models are selected around the medoid for ensemble smoother(ES).

The proposed distance can achieve improved reservoir characterization and history matching combined with ES. Also, this method helps to reduce uncertainty ranges of future oil and water productions, and decreases total simulation time by 75% with proper sampling of good 100 models.

Keywords: Distance, Ensemble smoother, Uncertainty quantification

Student Number: 2014−22728

Table of Contents

List of Tables

List of Figures

1. Introduction

As oil moves through reservoir rocks, the permeability is one of the crucial factors to produce oil. The most precise way to know the permeability distribution is to get many sample data. However, it is uneconomic in time and cost aspects. Instead, there are multiple models with equivalent probability generated using limited data available. These models are called ensemble members.

Ensemble members are created using limited data in exploration or early production stages. Thus, the uncertainty of ensemble is too high to predict reservoir properties correctly. To improve prediction, ensemble members are often applied to various reservoir characterization methods. This process is called ensemble-based reservoir characterization. Many studies have suggested ensemble-based reservoir characterization methods. There are two representative methods.

Ensemble Kalman filter(EnKF) is one of the popular methods. There are typical steps for EnKF(Fig. 1.1). EnKF was offered by Evensen(1994) to ocean dynamics for the first time. Nævdal et al.(2002) used EnKF for reservoir characterization, and provided that EnKF estimates reservoir permeability distribution reliably.

Evensen et al.(2007) proved that EnKF could be ineffective if it was applied to reservoir parameters with non-Gaussian distributions such as channel field. Therefore, Shin et al.(2010) proposed a non-parametric approach for EnKF to be applied to these fields.

With less than 100 ensembles, EnKF was revealed to give unreliable results with filter divergence problem(Wen and Chen, 2007). Thus, Jung and Choe(2012) suggested a streamline-assisted EnKF for covariance localization to get accurate results. This method estimated permeability field without overshooting or filter divergence. Also, Lee et al.(2013) grouped initial channel field models using Hausdorff distance, and applied a clustered covariance to improve EnKF results.

Although, many researchers have studied EnKF to solve typical problems of it, these methods are incapable of overcoming long simulation time in EnKF. That's because EnKF requires hundreds of ensembles to give trustworthy results. To avoid this problem, ensemble smoother(ES) was introduced.

ES is also one of the well-known ensemble-based reservoir characterization methods. Fig. 1.2 shows ES procedures. Skjervheim et al.(2011) first applied ES for history matching. They suggested that ES showed analogous results to EnKF provided that initial conditions had small perturbations.

Gervais et al.(2012) proposed repetition of ES twice showing similar results with EnKF in less simulation time. Lee et al.(2013) provided ES with a clustered covariance in channelized fields. With this method, they reduced uncertainty in initial ensembles and managed overshooting or filter divergence problems due to poor ensembles. By doing this, they could achieve channel reservoir characterization with only 5% simulation time of EnKF.

ES can produce reliable results with good initial models in less simulation time compared with EnKF. However, if initial models are not proper, the outcome from ES can be inaccurate. Thus, distance-based methods can improve this problem.

A distance represents dissimilarity between two ensemble members. By a distance-based sampling scheme, it is possible to choose more similar ensemble to a reference field and to reduce high uncertainty in ensemble. Combined with reservoir characterization methods, a sampling scheme can contribute to enhanced reservoir characterization and history matching.

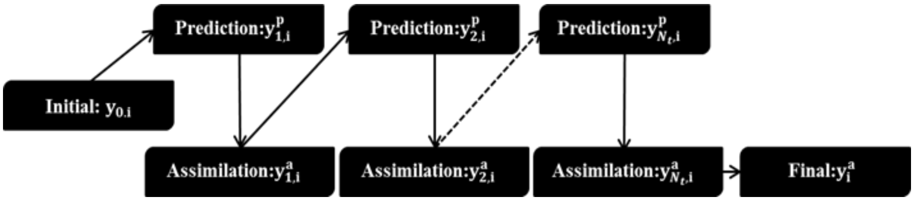

Fig. 1.1 – EnKF process(Kang, 2016).

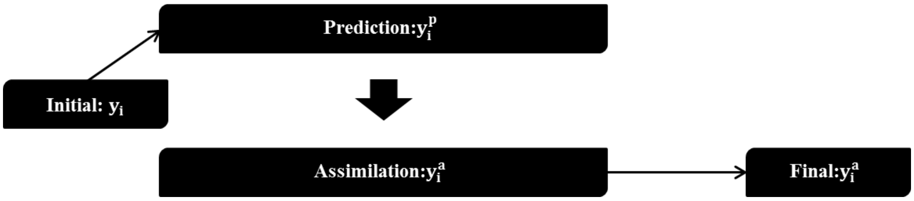

Fig. 1.2 – ES process(Kang, 2016).

Many distances have been suggested to select good reservoir models. For example, Dubuisson and Jain(1994) combined 6 distance measures via 4 ways, and compared the results. Suzuki and Caers(2008) measured the dissimilarity between geologic models with channel by Hausdorff distance. However, these distances are calculated using entire permeability data of ensembles. If they are applied to large-sized fields, the calculation can be encumbered. Kang et al.(2016) used singular value decomposition(SVD) and improved ES by sampling better initial ensembles. Nevertheless, it is difficult to understand the principle of SVD intuitively.

Scheidt and Caers(2009a) defined a distance as a difference of field oil rates at two time points. Also, Scheidt and Caers(2009b) obtained a distance matrix by considering cumulative oil and water productions during total production period. Jin et al.(2011) defined a distance as difference of injected stream between ensembles. Lee et al.(2015) proposed a distance according to a difference of oil sand percentage in rectangles expanded from an injector. Park et al.(2015) analyzed travel time of streamlines in ensembles and decided the difference of generalized travel time as a distance.

These suggested distances require model simulation of all initial ensembles before sampling, which causes excessive time. Therefore, it is necessary to define an effective distance without initial simulation for all ensemble members.

In this paper, a distance is defined as a difference in correlation coefficient between two reservoir models by applying two spatial patterns. These patterns can consider representative permeability distributions in reservoir models. According to the distance, proper models are selected as new initial models for enhanced ES results.

2. Methodologies

2.1 Definition of a distance from spatial patterns

Permeability data around wells are important to predict reservoir behaviors. Therefore, two spatial patterns are suggested to consider key permeability data in typical nine spot well locations. The first pattern, called 1-line case, consists of 21 by 1 permeability data at the center of x and y directions(Fig. 2.1a). The second pattern, called cross case, consists of the 1-line plus two diagonal directions(Fig. 2.1b). From the comparison of these two cases, it is plausible to analyze whether it is good or not to consider permeability data from the injector to all producers.

To compare difference of each ensemble, correlation coefficients are computed between permeability data acquired from the two spatial patterns. The Eq. for correlation coefficient, Corr(A, B) is Eq. 2.1. Then, the distance comes out as L2-norm of the correlation coefficient subtracted from 1(Eq. 2.2).

$$\boldsymbol{Corr(A,B)} = \frac{\sum(\boldsymbol{A_i}-\bar{\boldsymbol{A}})(\boldsymbol{B_i}-\bar{\boldsymbol{B}})}{\sqrt{\sum(\boldsymbol{A_i}-\bar{\boldsymbol{A}})^2}\sqrt{\sum(\boldsymbol{B_i}-\bar{\boldsymbol{B}})^2}} \tag{2.1}$$

$$\boldsymbol{Distance(A,B) = \sqrt{(1 - Corr(A,B))^2}} \quad (2.2)$$

where, A_i and B_i are the i−th data obtained from spatial patterns of A and B ensembles, respectively.

Fig. 2.2 is an example of the distance based sampling scheme procedure in this study. By the simple 1−line spatial pattern, the distance between two models can be calculated. After computing all the distances among 4 models shown, they are presented on 2D−plane to illustrate reservoir models as points. Then, clustering is conducted to divide them into several groups. Finally, models are chosen around a group with the least production difference from a reference field.

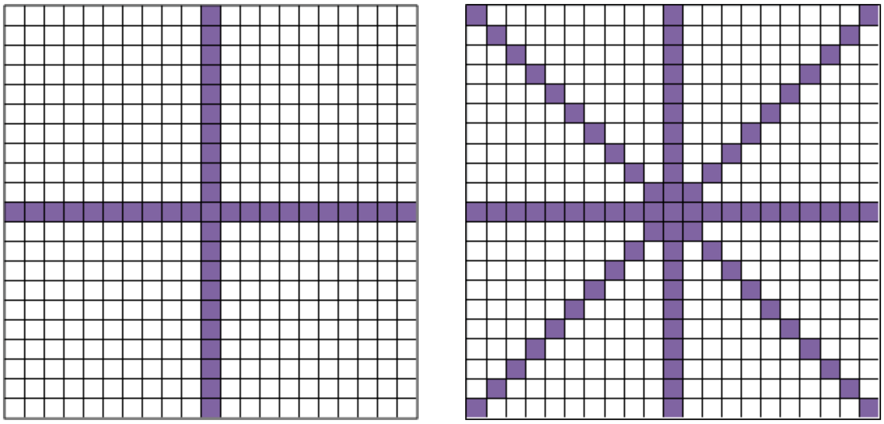

(a) 1-line

(b) Cross

Fig. 2.1 – Two spatial patterns suggested in this study.

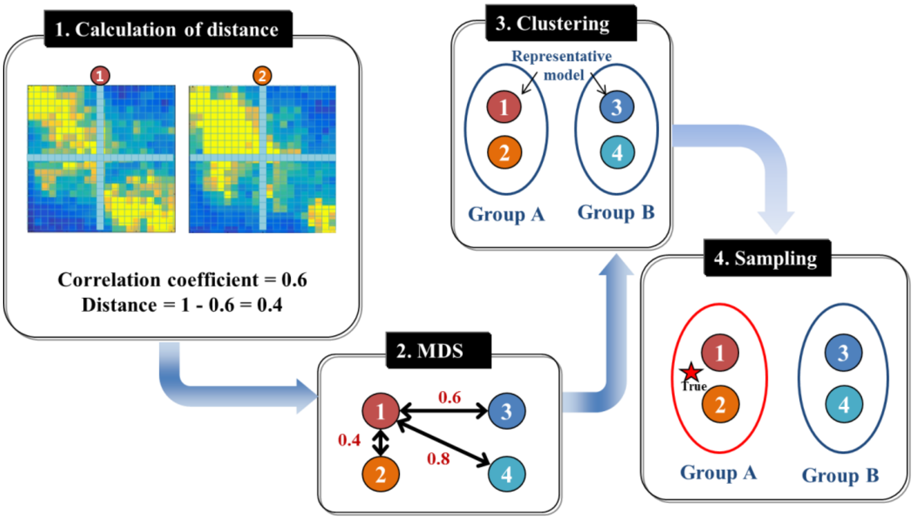

Fig. 2.2 – Distance based sampling scheme procedure.

2.2 Multi−dimensional scaling

Multi−dimensional scaling(MDS) is one of methods to project data on low dimension according to dissimilarity between data. If the dissimilarity is high, they are located on MDS space far away each other(Fig. 2.3). On the other hand, they are located closely when the dissimilarity is low. Before using MDS, it is crucial to define a dissimilarity called distance, and 4 terms are necessary as below(Jin, 2011).

- Negative value cannot be a distance between two data.
- The distance between one point and itself must be zero, and there is no zero between two different data points.
- The distance between data x and y is same as the distance between data y and x.
- In a triangle composed of 3 points on space, the sum of two sides is always greater than or equal to the third.

Fig. 2.3 – The depiction of data from 3D-space on 2D-plane.

The best advantage of MDS is that it enables people to present the relationship between two data on two or three dimensions(3D). Also, the relationship between data points on low-dimension can be easily visualized and analyzed intuitively by MDS. Thus, MDS can be helpful to categorize data based on similar characteristics and to examine data clustering results visually.

The MDS principle has been widely applied to many fields because it uses the distance, not the data directly. Sometimes, people might get results from an alternative model, not the data itself. In this case, they can compare results from alternative models and investigate relationships between data using MDS.

By MDS, it is feasible to find new dimension where data exists. Also, if one knows only dissimilarity between data, data analysis like a clustering is still achievable. That's because the dimension and coordinates of data are obtainable. Generally, MDS can be conducted using linear algebraic methods without iterative algorithm. The procedure is explained as below.

- Square each element of distance matrix(Eq. 2.3).

$$\boldsymbol{P}^{(2)} = [\boldsymbol{p}^2] \tag{2.3}$$

- Generate a centering matrix J using Eq. 2.4 as below.

$$\boldsymbol{J} = \boldsymbol{I} - \frac{1}{n}\mathbf{1}\mathbf{1} \quad (2.4)$$

where, n means the total number of objects, and I is the unit matrix. Also, 1 is the column-vector of n ones.

- By the matrix J, the matrix B can be computed as in Eq. 2.5.

$$\boldsymbol{B} = -\frac{1}{2}\boldsymbol{J}\boldsymbol{P}^{(2)} \quad (2.5)$$

- Calculate the m largest eigenvalues, λ_1 , $\cdots, \lambda_m$ and corresponsive eigenvectors, e_1, $\cdots$, e_m. The m means the number of low dimension.
- A coordinate matrix X can be explained using Eq. 2.6 to present n objects on m-dimensional space.

$$\mathbf{X} = \mathbf{E_m}\mathbf{\Lambda_m^{1/2}} \quad (2.6)$$

where, $\mathrm{E_m}$ means the matrix of m eigenvectors and Λ_m is the diagonal matrix composed of m eigenvalues from B.

2.3 K−medoids clustering

Clustering is used to find out structures among data and to divide the data into several groups. People can understand the characteristics of data easily by clustering. Therefore, it is widely employed in classification, prediction, or inducement of control rules in pattern recognition, image treatment, data−mining, and so on.

K−medoids clustering is one of widely applied clustering methods. It assigns data which have N−attributes on N−dimensional locations, and divides them into K−clusters to understand characteristics of data. The location of medoids is significant because data are assigned to the closest cluster according to the distance from each medoid. The procedure of K−medoids is shown in Fig. 2.4.

First, select K data randomly for K clusters, and designate them as medoids of each group. Then, include the data closest to a medoid into the medoid's group by measuring linear distance. After that, decide new medoids based on the average of data from each dimension as the third step. The linear distances between data and medoids are estimated, and the data are classified as new group if the sum of linear distances is smaller than the prior one. The procedure from the second to third is repeated until the locations of medoids are not changed as the fourth step.

The initial setup for medoid has huge influence on clustering results. Thus, appropriate repetition is essential to get the clustering results with the least linear distance between data and medoid.

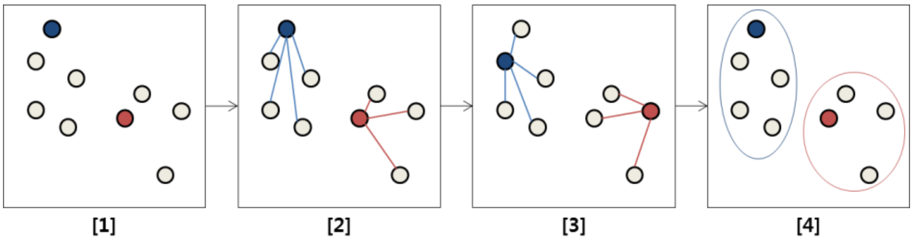

Fig. 2.4 – K-medoids clustering procedure.

2.4 Ensemble smoother

To be applied to ES, the i−th ensemble is expressed by state vector, y_i as in Eq. 2.7.

$$\boldsymbol{y_i} = \begin{bmatrix} \boldsymbol{m^s} \\ \boldsymbol{m^d} \\ \boldsymbol{d} \end{bmatrix}, \boldsymbol{i} = \boldsymbol{1}, \boldsymbol{N_e} \tag{2.7}$$

where, N_e is the total number of ensemble applied to ES, m^s is the static parameters, m^d is the dynamic parameters, and d is the observed data. At first, ES forecasts observed data of initial ensemble members by forward simulation. Next, ES assimilates initial ensemble members using entire accessible data and Kalman gain, K. Kalman gain can be calculated by minimizing the estimated error covariance, C_Y. Eqs. 2.8 and 2.9 show specific calculation in the assimilation step.

$$\boldsymbol{y_i^a} = \boldsymbol{y_i^p} + \boldsymbol{K}(\boldsymbol{d_i} - \boldsymbol{H}\boldsymbol{y_i^p}) \tag{2.8}$$

$$\boldsymbol{K} = \boldsymbol{C_Y^p}\boldsymbol{H^T}(\boldsymbol{H}\boldsymbol{C_Y^p}\boldsymbol{H^T} + \boldsymbol{C_D})^{-1} \tag{2.9}$$

where, the superscripts a and p mean the assimilation step and the priori state vector, respectively. Also, H is the measurement operator. C_D indicates the measurement error covariance.

3. Results and discussions

In this study, initial 400 ensemble members are generated by sequential Gaussian simulation using known permeability data in 9 wells. The location of these wells is on 21 by 21 grids as a typical nine spot spacing. After proper ensemble selection by the distance−based sampling scheme, ES is applied to them. The assimilation period is 500 days, and the total production time is 1,000 days. For showing versatility of this method, two types of fields are used. More detailed simulation setup is shown in Table 3.1.

Table 3.1 – Reservoir and simulation conditions

Well location, grid coordinate	(2, 2),(2, 11),(2, 20),(11, 2),(11, 11),(11, 20),(20, 2),(20, 11),(20, 20)
Known data at well locations of field type 1, ln(md)	5.4, 3.3, 5.2, 3.1, 3.2, 3.1, 3.2, 3.3, 3.0
Known data at well locations of field type 2, ln(md)	3.1, 3.5, 5.0, 3.6, 4.5, 3.5, 5.1, 3.4, 3.0
Assimilation time, days	100, 200, 300, 400, 500
Total simulation period, days	1,000
Observed data types	Well oil production rates
Porosity, fraction	0.20
Initial water saturation, fraction	0.25
Initial reservoir pressure, psia	2,000

3.1 Field with high permeability at the side corners

This field shows high permeability zone at the left side(case Ⅰ). Figs. 3.1 and 3.2 show the reference field and averaged initial 400 ensemble members to illustrate permeability distributions. Most of permeabilities are low except for the corners of the left side. For the initial 400 ensemble members, Figs. 3.3 and 3.4 indicate high uncertainty in productions from the members.

The red lines are productions from the reference field, and the blue lines are averaged productions of the initial 400 ensemble. The blue lines do not follow the trend of the red lines properly. The gray lines are productions from each ensemble member. The band width of these gray lines is too wide to predict the production trend of the reference field.

Before checking out selected ensemble from spatial patterns, randomly selected 50 ensemble members are presented in Fig. 3.5. This case will be called random case. There are three ensemble members from the random case(Fig. 3.6). They are randomly selected to look into the permeability distribution of ensemble members, which are affiliated to the random case. The high permeability connection between the injector and producers at the left corner is not considered properly in these ensemble members.

By sampling scheme using the 1−line, Fig. 3.7 illustrates the initial 400 ensemble members on 2D−plane. Also, 50 ensemble members are selected for a new initial ensemble applied to ES. The average of the selected 50 ensemble members is presented in Fig. 3.8. This case does not consider the connectivity of high permeability zone at the left corner like the random case.

Fig. 3.9 displays three randomly selected ensemble members which belong to the 1−line case. Even though the connectivity of high permeability appears in the third one, the other ensemble members seem not to have the similar permeability distribution of the reference field.

As same as the 1−line case, 50 ensemble members are presented on 2D−plane, which are chosen among the initial 400 ensemble members using the cross pattern (Fig. 3.10). Fig. 3.11 gives averaged permeability distribution of the selected 50 ensemble members and its histogram from the cross case. Unlike the other cases, the permeability distribution shows connectivity from the left corner to the injector. Also, Fig. 3.12 presents three ensemble members randomly selected from the chosen 50 ensemble of the cross case. Compared with the other cases, the connection in high permeability zone stands out among these ensemble members. That's because the cross case can capture the permeability difference between ensemble members in diagonal directions.

To analyze productions, box plots on cumulative oil and water productions are drawn as in Fig. 3.13. The horizontal red lines mean cumulative oil and water productions from the reference field. The box plots from the cross case are the closest to the reference field in oil and water productions. Because the 1-line pattern can't investigate high permeability zone at corners, the box plots of this case do not include the reference field between the first and third quartiles. The random case also gives poor prediction for productions.

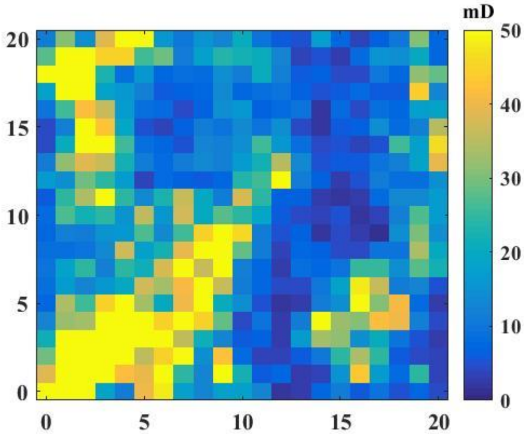

(a) Reference field

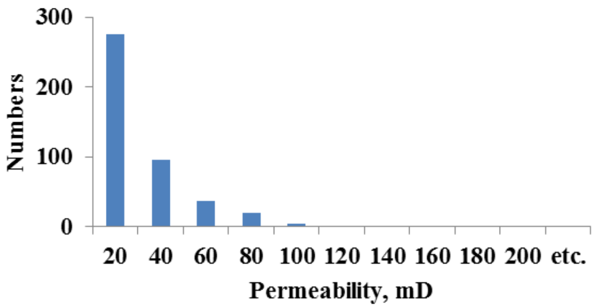

(b) Histogram of permeability

Fig. 3.1 – Reference field of case Ⅰ.

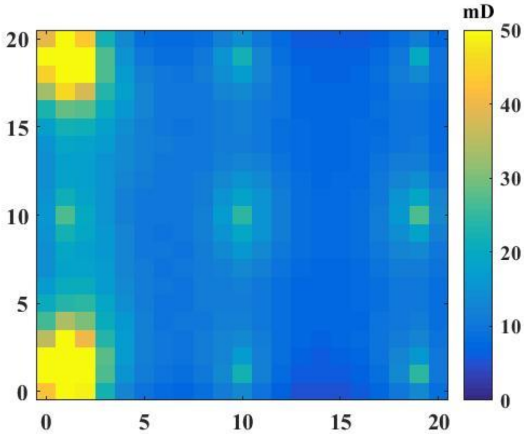

(a) The average permeability

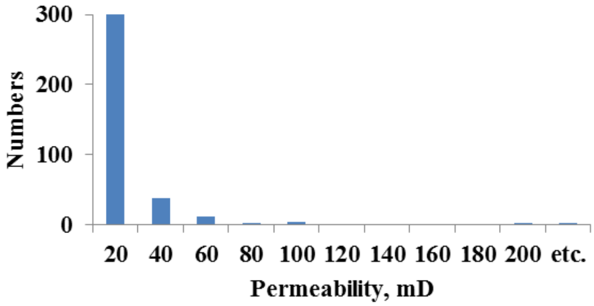

(b) Histogram of permeability

Fig. 3.2 – Initial 400 ensemble members of case Ⅰ.

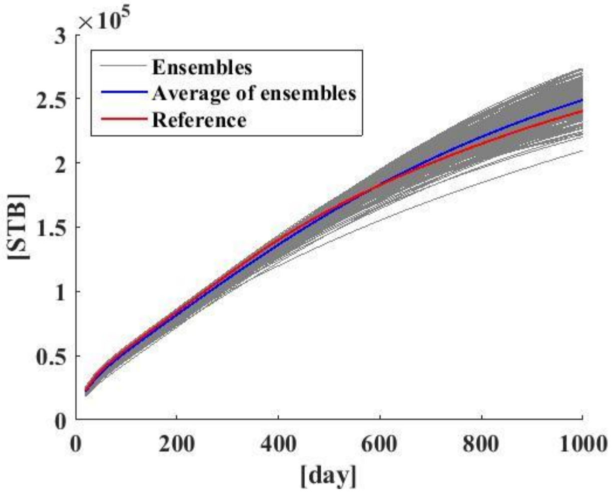

(a) Oil

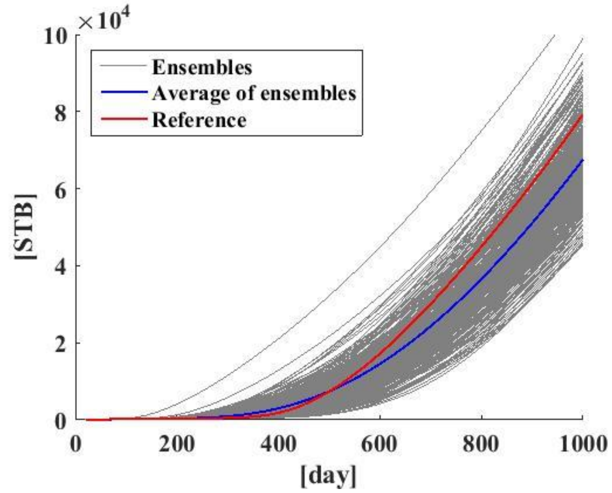

(b) Water

Fig. 3.3 – Cumulative oil and water productions of the initial 400 ensemble members.

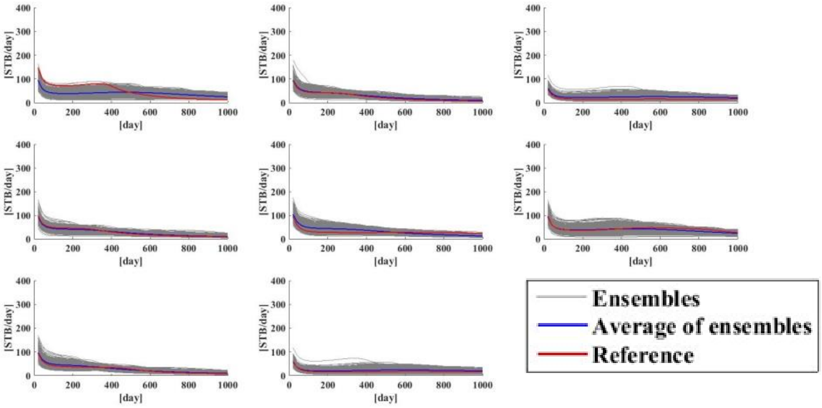

(a) Oil rates

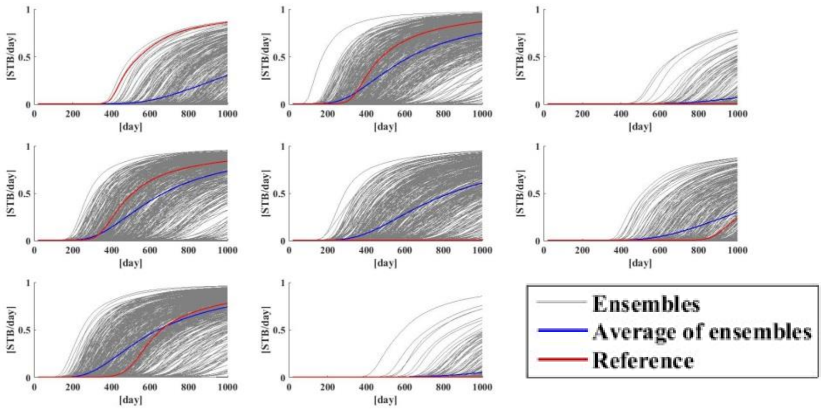

(b) Water rates

Fig. 3.4 – Well production rates of the initial 400 ensemble members.

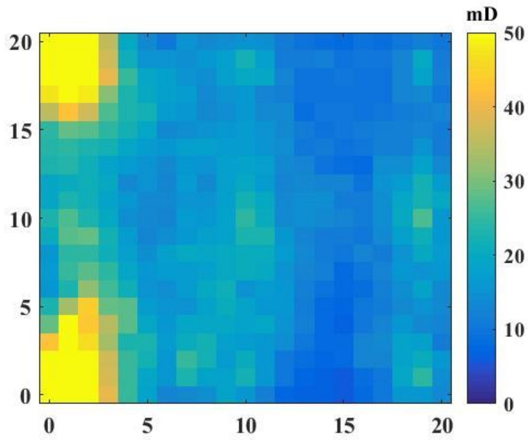

(a) The average permeability

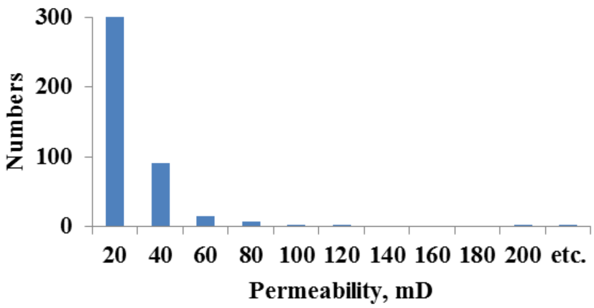

(b) Histogram of permeability

Fig. 3.5 – Randomly selected 50 ensemble members from case Ⅰ.

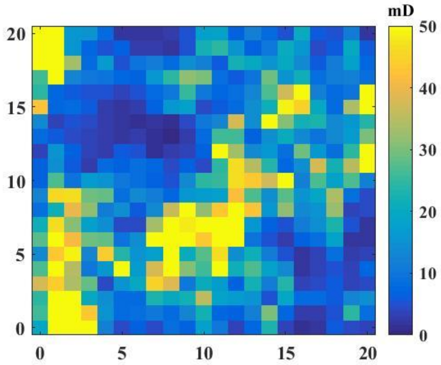

(a) First

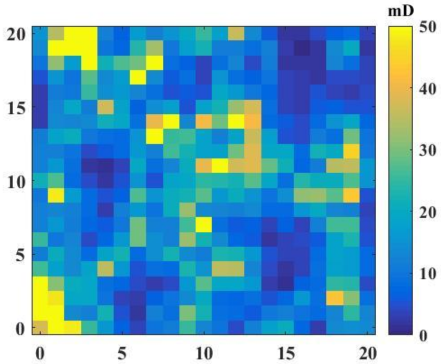

(b) Second

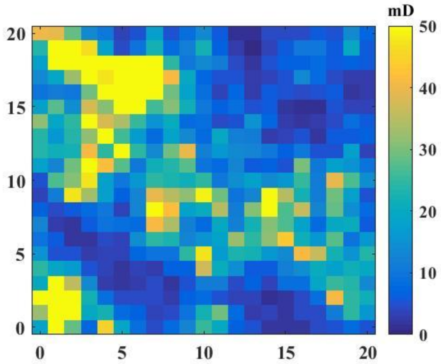

(c) Third

Fig. 3.6 – Three examples of ensemble members from the random case.

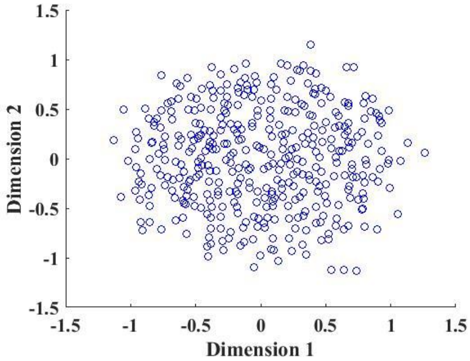

(a) MDS

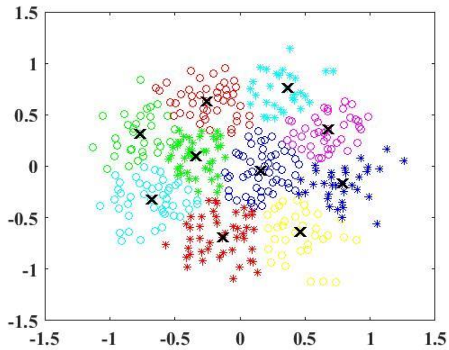
(b) K-medoids clustering

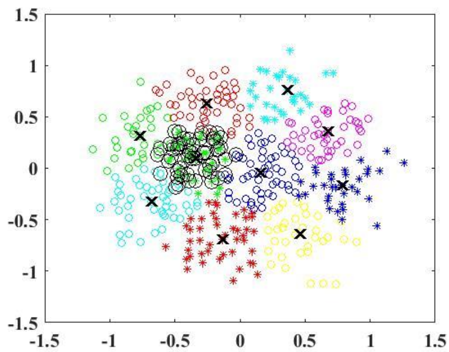
(c) Selected 50 ensembles on 2D-plane

Fig. 3.7 – Sampling scheme results by the 1-line pattern from case Ⅰ.

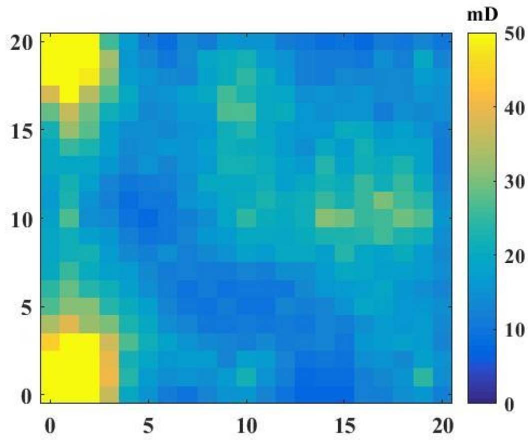

(a) The average permeability

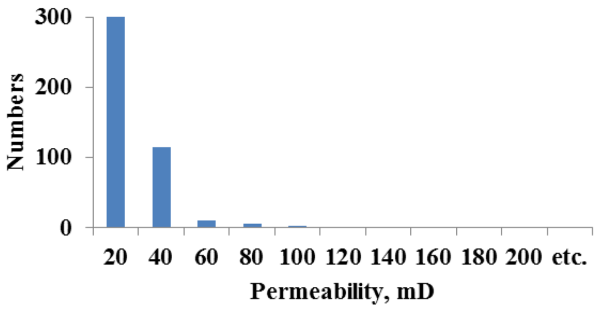

(b) Histogram of permeability

Fig. 3.8 – Selected 50 ensemble members by the 1-line pattern from case Ⅰ.

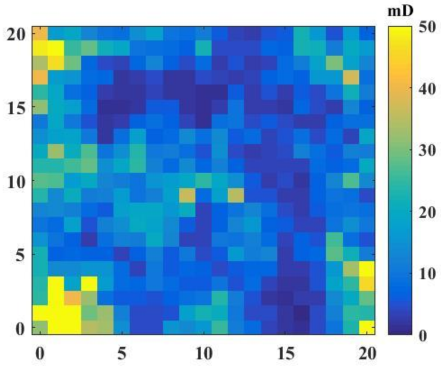

(a) First

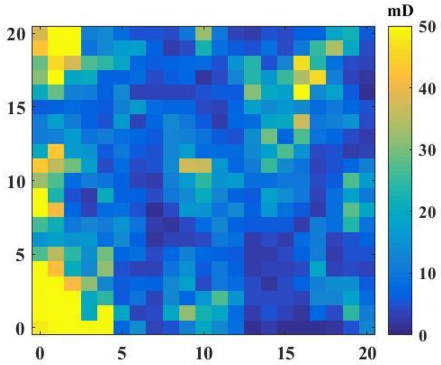

(b) Second

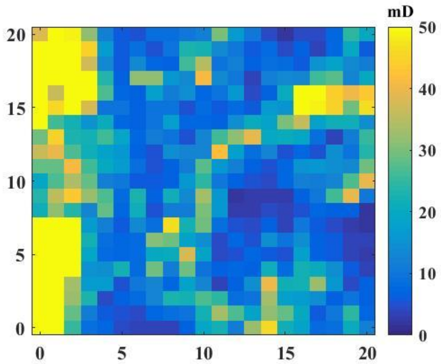

(c) Third

Fig. 3.9 – Three examples of ensemble members from the 1-line case.

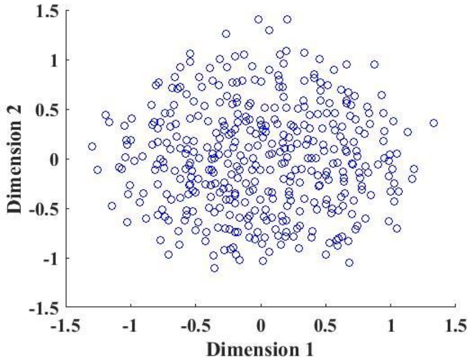

(a) MDS

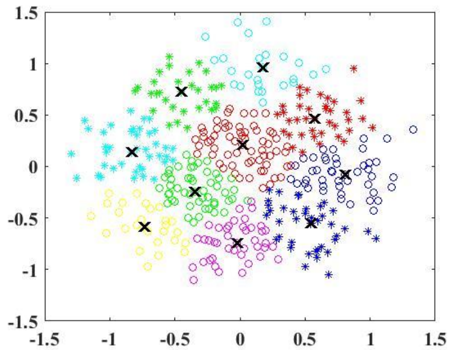

(b) K-medoids clustering

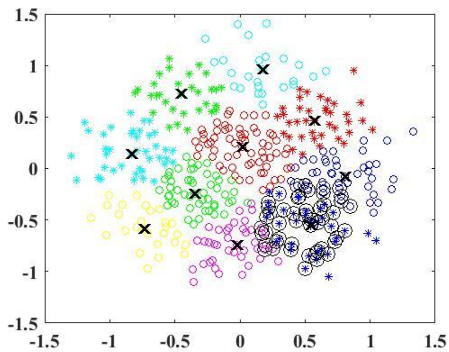

(c) Selected 50 ensembles on 2D-plane

Fig. 3.10 – Sampling scheme results by the cross case from case Ⅰ.

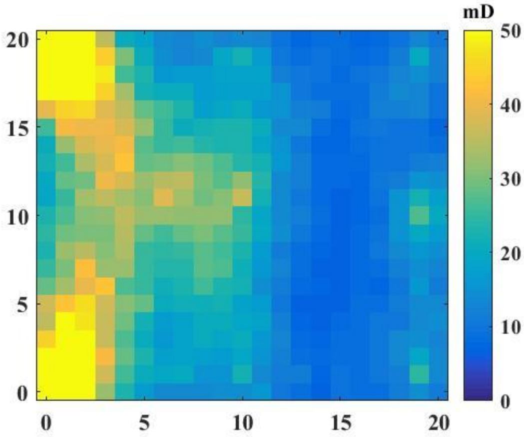

(a) The average permeability

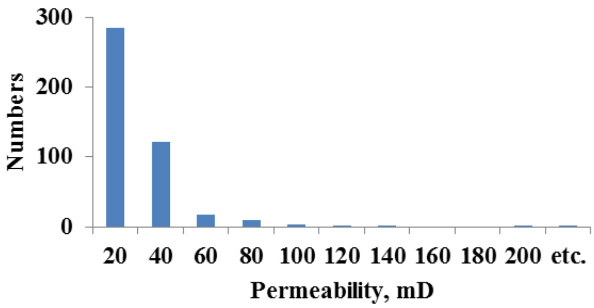

(b) Histogram of permeability

Fig. 3.11 – Selected 50 ensemble members by the cross pattern from case Ⅰ.

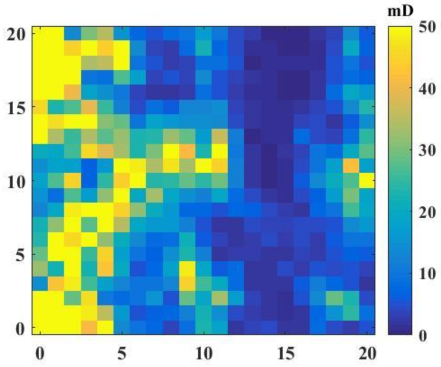

(a) First

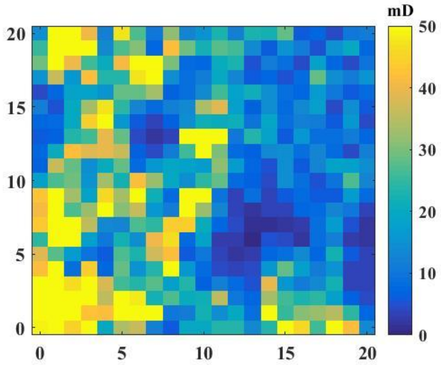

(b) Second

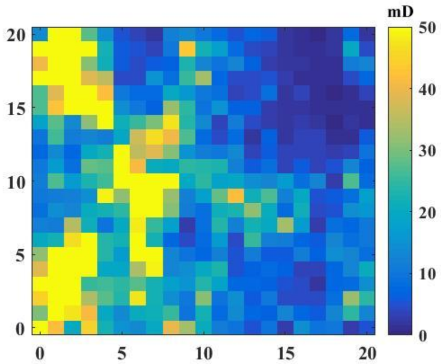

(c) Third

Fig. 3.12 – Three examples of ensemble members from the cross case.

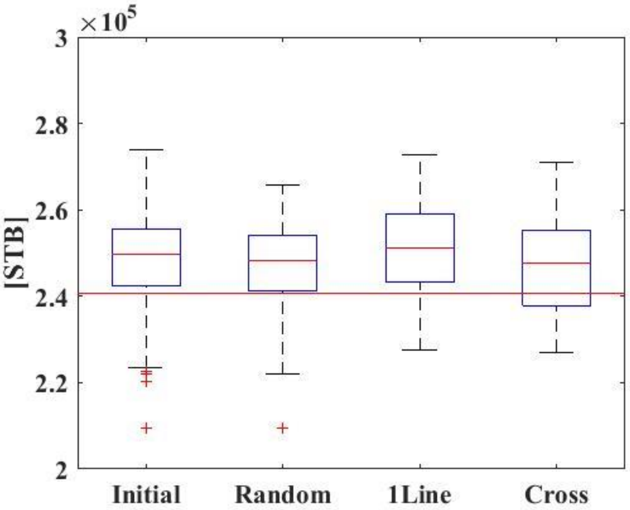

(a) Oil

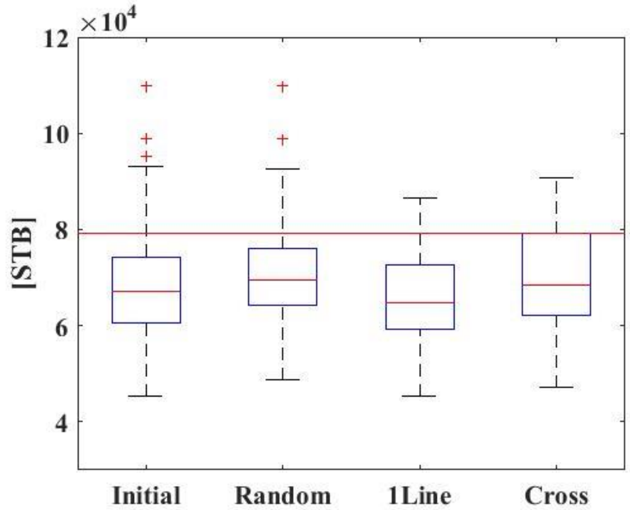

(b) Water

Fig. 3.13 – Box plots for cumulative oil and water productions from the initial 400 ensemble, random, 1-line, and cross cases before ES in case Ⅰ.

Fig. 3.14 shows updated 400 ensemble members. The ES results using the random case and two spatial patterns are presented from Figs. 3.15 to 3.17. Because of many ensemble members, the histogram of the 400 ensemble members follows the permeability distribution trend stably. Also, the cross case estimates the reference field well using just 50 ensemble members.

Ensemble-based reservoir characterization typically requires over 100 ensemble members for reliable results. Thus, the random and 1-line cases show overshooting problem which means that estimated permeability values are excessively higher than those of the reference field. Therefore, the random and 1-line cases are poor at sampling good ensemble members compared with the cross case.

Also, Fig. 3.18 shows box plots for cumulative oil and water productions after ES from all cases. The cross case gives dependable results with better uncertainty assessment compared with the other cases. Except for the 400 and cross cases, there are filter divergence problems. Therefore, it is difficult to predict future productions by the 1-line and random cases.

The total simulation time is shown in Table 3.2. The cross case can be conducted with over 80% time reduction compared with the case using 400 ensemble members, and gives good reservoir characterization. The computer specs used in this study are Intel R Core TM i5−3570 CPU @ 3.4o GHz and RAM is 8.00 GB.

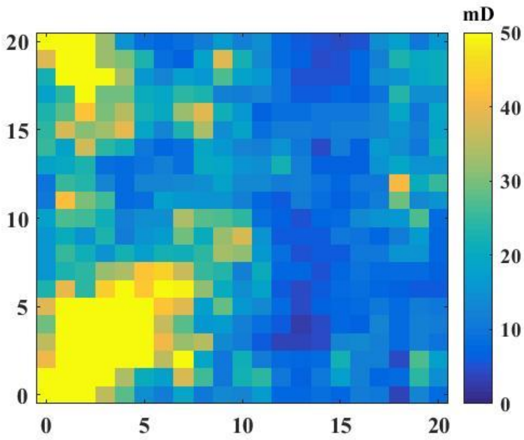

(a) The average of updated permeability

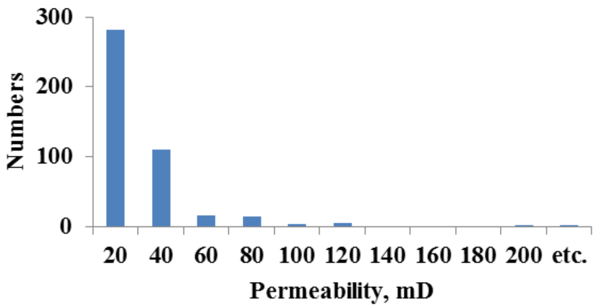

(b) Histogram of permeability

Fig. 3.14 – Updated 400 ensemble members after ES in case Ⅰ.

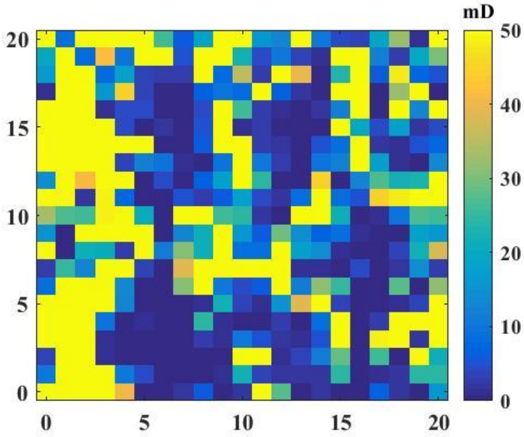

(a) The average of updated permeability

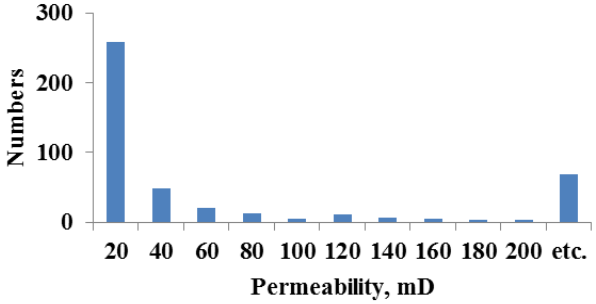

(b) Histogram of permeability

Fig. 3.15 – Updated 50 ensemble members from the random case after ES in case Ⅰ.

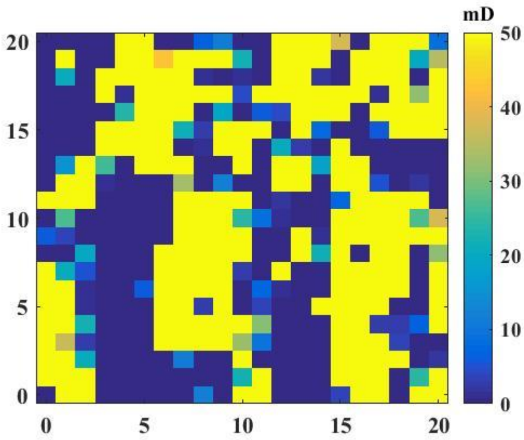

(a) The average of updated permeability

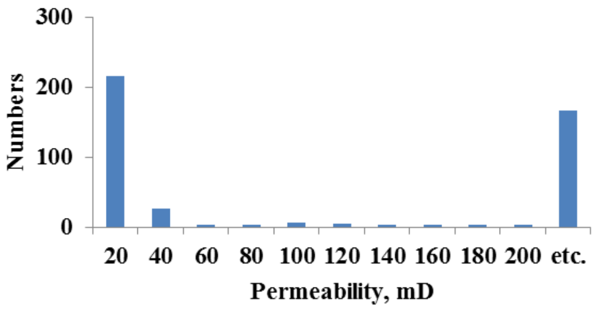

(b) Histogram of permeability

Fig. 3.16 – Updated 50 ensemble members from the 1-line case after ES in case Ⅰ.

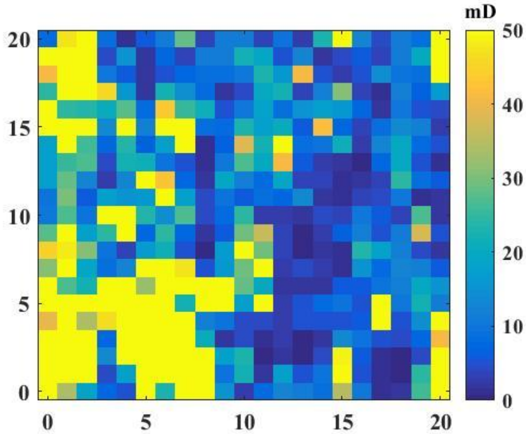

(a) The average of updated permeability

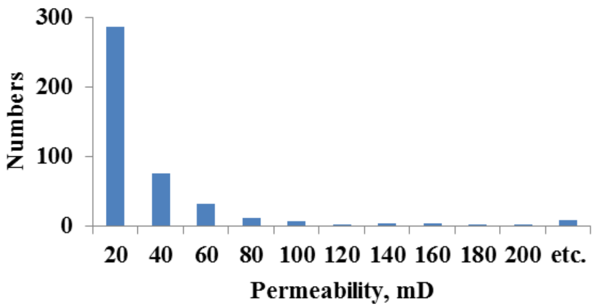

(b) Histogram of permeability

Fig. 3.17 – Updated 50 ensemble members from the cross case after ES in case Ⅰ.

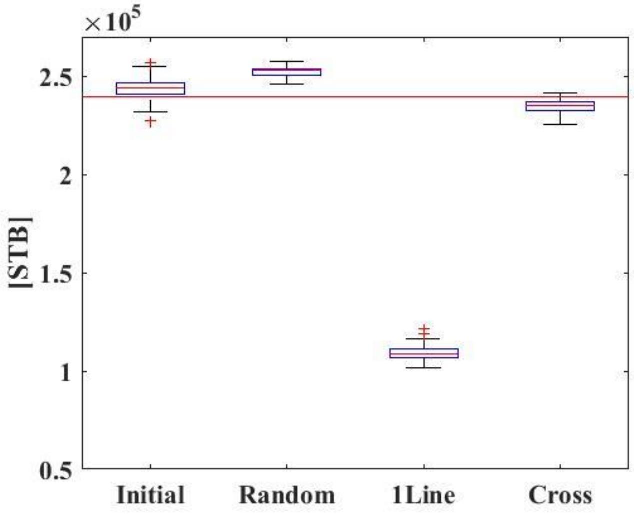

(a) Oil

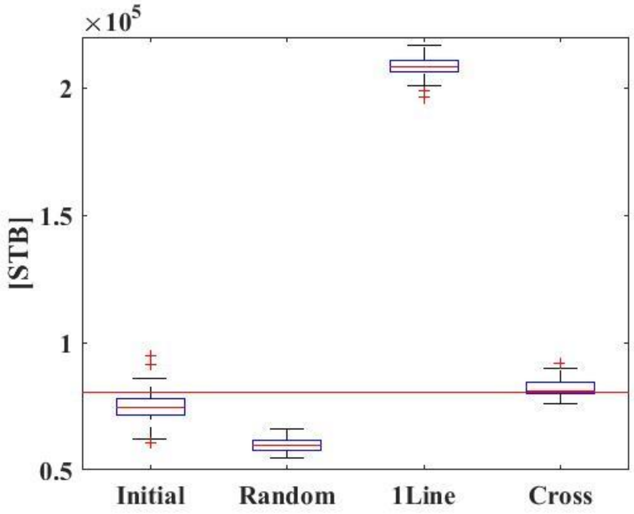

(b) Water

Fig. 3.18 – Box plots for cumulative oil and water productions from the 400 ensemble, random, 1-line, and cross cases after ES in case Ⅰ.

Table 3.2 – Total simulation time and its reduction for case Ⅰ.

	Initial	Random	One-line	Cross
Time, min	90	10	10	10
Reduced time, %	-	88	88	88

3.2 Field with high permeability in diagonal direction

Fig. 3.19 shows a reference field with high permeability distribution in diagonal direction(case Ⅱ). Fig. 3.20 presents the averaged permeability distribution of the initial 400 ensemble and its histogram. Because the feature of high permeability zone is evident in the middle of the field, the connection of the zone can be easily identified in x and y directions. Therefore, different from case Ⅰ, the 1-line case also discovers characteristics of permeability in ensemble members. This time, total 100 ensemble members are chosen to provide enough initial models for stable ES results.

Fig. 3.21 shows the random case composed of 100 ensemble members. To confirm opted ensemble members individually, three ensemble members are chosen as shown in Fig. 3.22. Although there might be ensemble comparable to the reference field, the second and third ensemble members have lower permeability values in the middle of the diagonal direction compared with that of the reference field.

After sampling by MDS and K-medoids clustering, Fig. 3.23 illustrates the average of the selected 100 ensemble members from the 1-line case. The shape of high permeability zone appears like the reference field. Fig. 3.24 indicates the randomly chosen three ensemble members from the 1−line case. In the third one, there is a disconnection of high permeability unlike the reference field.

Likewise, 100 ensemble members are selected by the cross pattern and presented in Fig. 3.25. The shape of histogram is almost the same as the 1−line case. However, in Fig. 3.26, the high permeability zone is described better than that of the 1−line by analysis of three of the selected members. That is because the cross case can grasp out diagonal permeability distributions. This sampling affects the production prediction as well(Fig. 3.27). The productions from the cross case are closest to the reference field. Also, the uncertainty range is decreased a lot compared to the initial one.

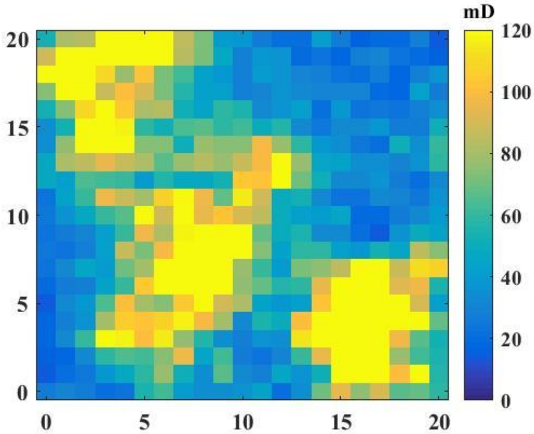

(a) Reference field

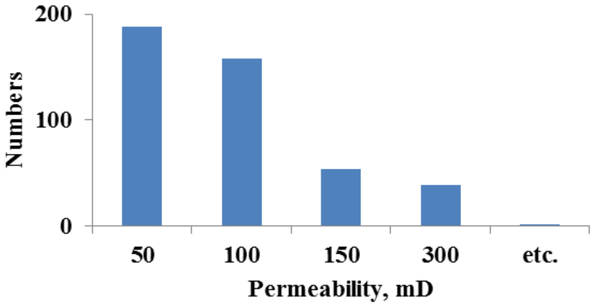

(b) Histogram of permeability

Fig. 3.19 – Reference field of case Ⅱ.

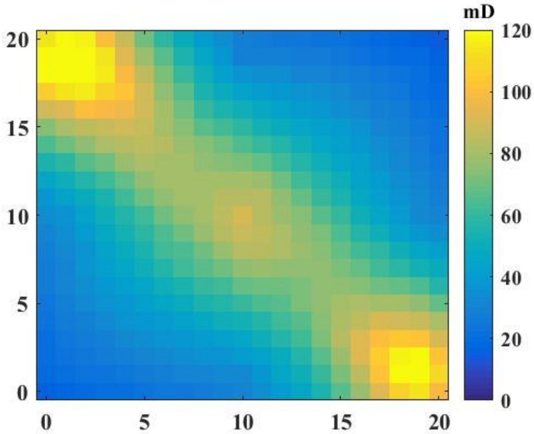

(a) The average permeability

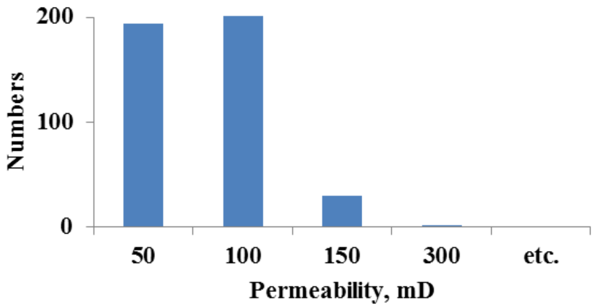

(b) Histogram of permeability

Fig. 3.20 – Initial 400 ensemble members of case Ⅱ.

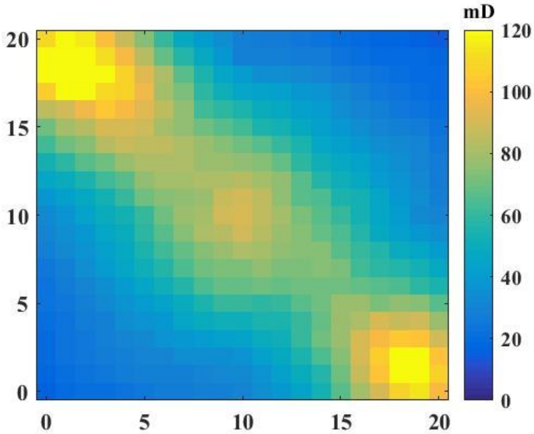

(a) The average permeability

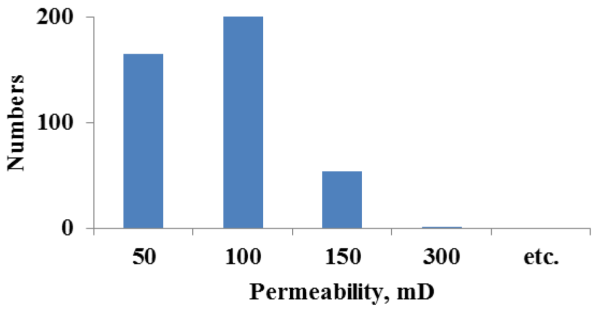

(b) Histogram of permeability

Fig. 3.21 – Randomly selected 100 ensemble members from case Ⅱ.

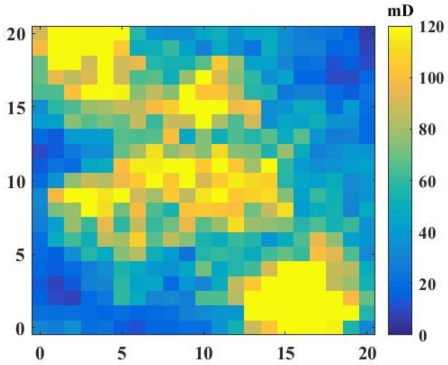

(a) First

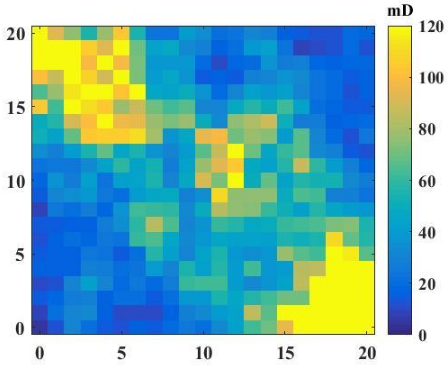

(b) Second

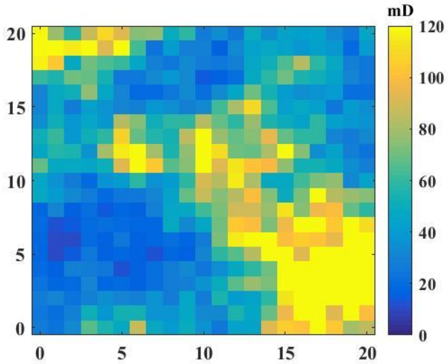

(c) Third

Fig. 3.22 – Three examples of ensemble members from the random case.

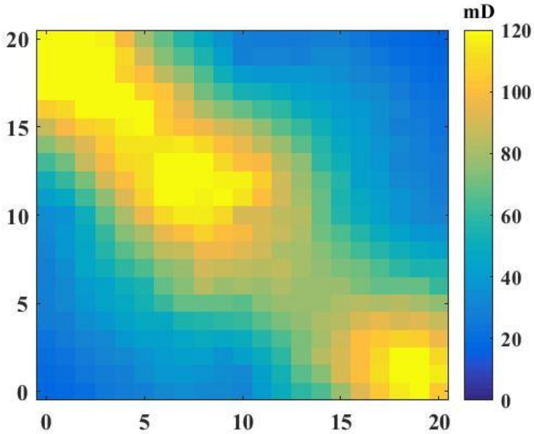

(a) The average permeability

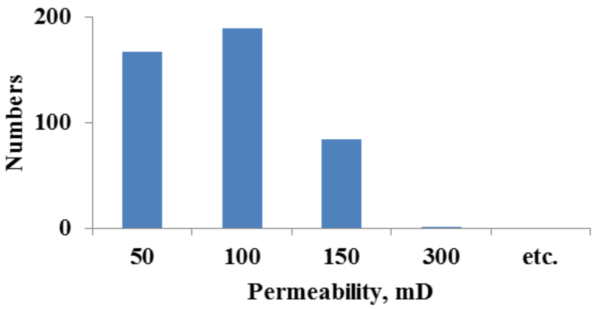

(b) Histogram of permeability

Fig. 3.23 – Selected 100 ensemble members

by the 1-line pattern from case Ⅱ.

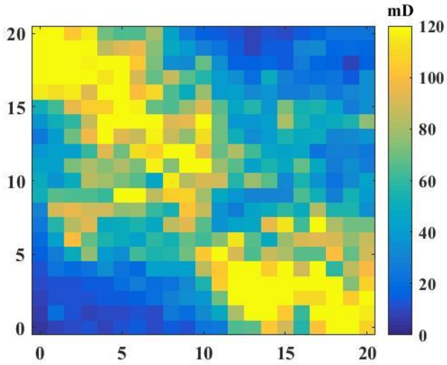

(a) First

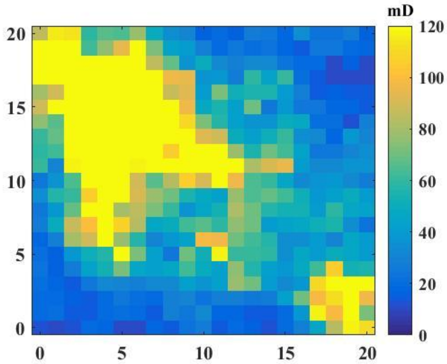

(b) Second

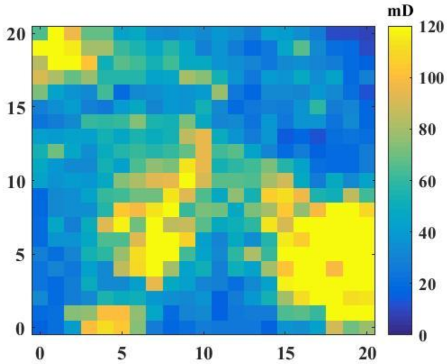

(c) Third

Fig. 3.24 – Three examples of ensemble members from the 1-line case.

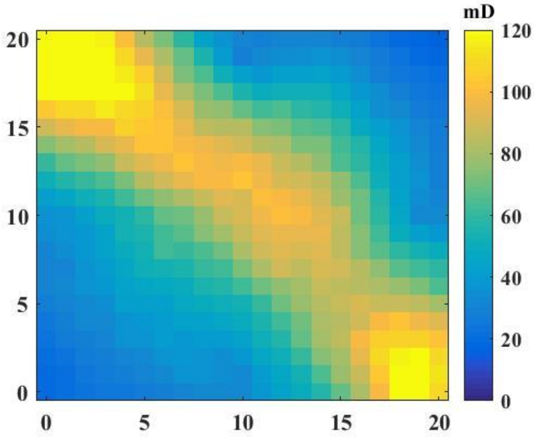

(a) The average permeability

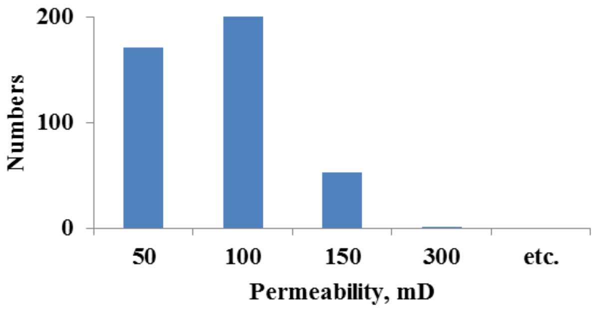

(b) Histogram of permeability

Fig. 3.25 – Selected 100 ensemble members

by the cross pattern from case Ⅱ.

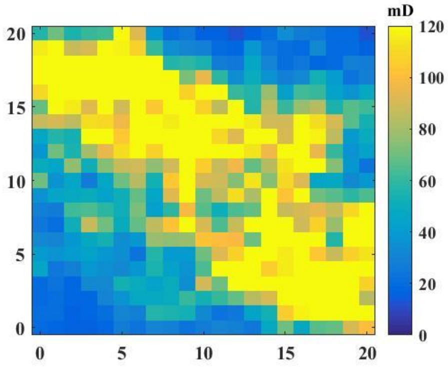

(a) First

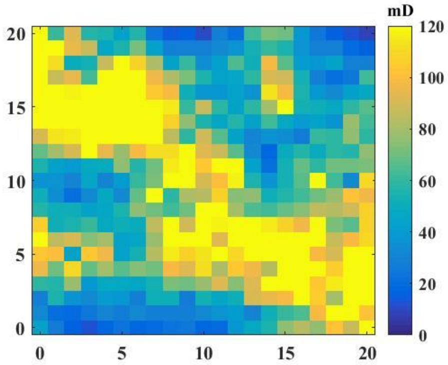

(b) Second

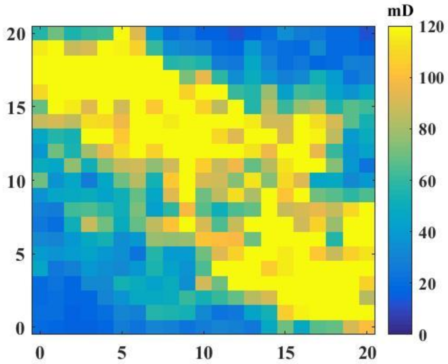

(c) Third

Fig. 3.26 – Three examples of ensemble members from the cross case.

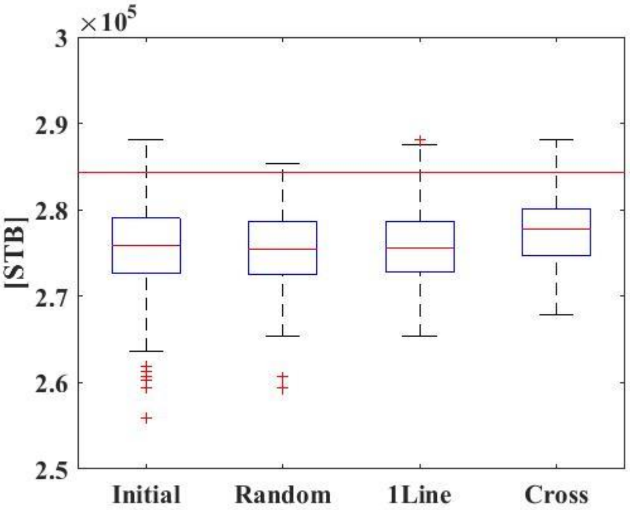

(a) Oil

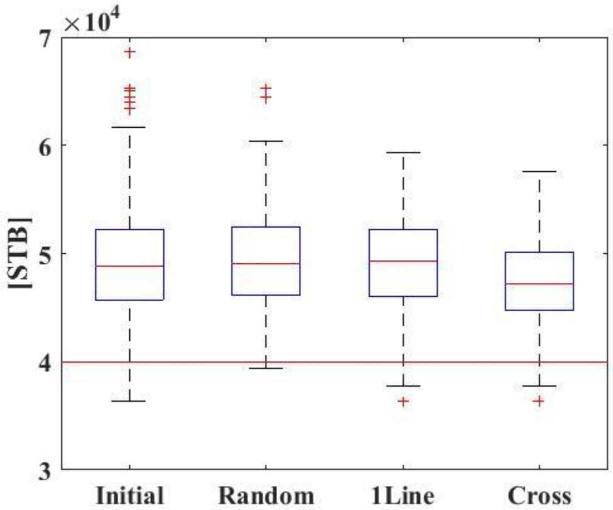

(b) Water

Fig. 3.27 – Box plots for cumulative oil and water productions from the initial 400 ensemble, random, 1-line, and cross cases before ES in case Ⅱ.

ES is applied to the initial 400 and selected 100 ensemble members from the random, 1−line, and cross cases. There are updated 400 ensemble members(Fig. 3.28). Even though the 400 ensemble case uses a lot of ensemble members, the updated result is not well−matched to the reference field. The results using spatial patterns show more improved reservoir characterization than the initial and random cases.

Compared with the poor results from the initial and random cases(Figs. 3.28 and 3.29), the histograms from the 1−line and cross cases are similar to that of the reference field(Figs. 3.30 and 3.31). Looking carefully, the cross case predicts the reference field better than the 1−line case in the high permeability over 150 mD of its histogram.

Fig. 3.32 shows box plots of cumulative oil and water productions after ES application. The cross case gives the best results among all the cases. Although the 1−line case shows decreased uncertainty range compared with the initial and random cases, it is unreliable because of biased estimation on water productions.

Therefore, it is apparent that the cross case works more properly for the reservoir characterization than the other cases. Table 3.3 shows comparison of total simulation time from all the cases. By the cross cases with 100 ensemble members, credible reservoir characterization is accomplished with almost

75% simulation time reduction. The computer of this study is Intel R Core TM i5-3570 CPU @ 3.4o GHz and RAM is 8.00 GB.

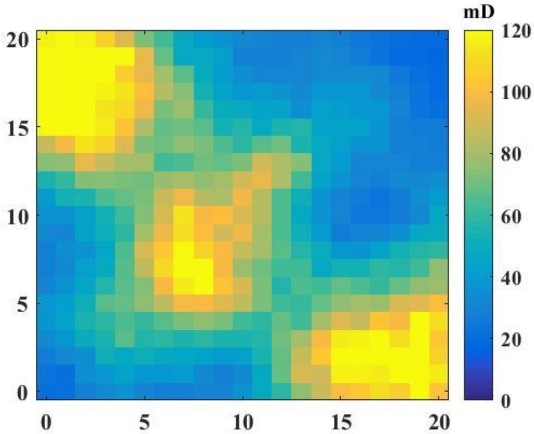

(a) The average of updated permeability

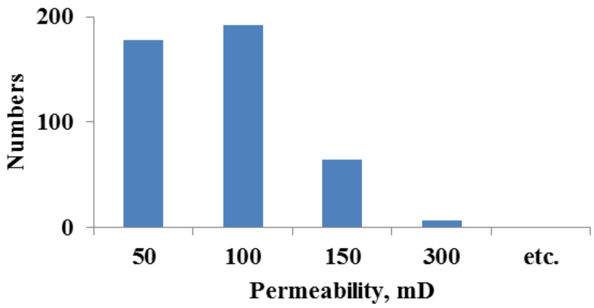

(b) Histogram of permeability

Fig. 3.28 –Updated 400 ensemble members after ES in case Ⅱ.

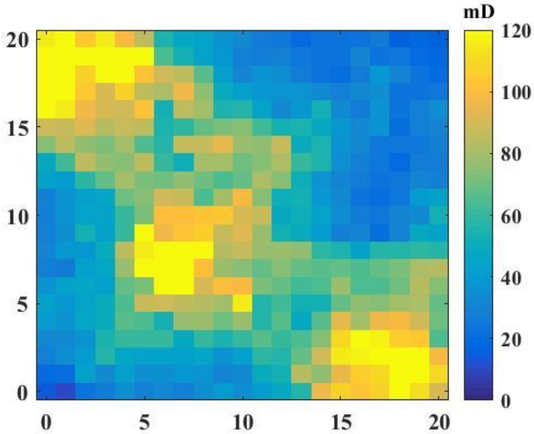

(a) The average of updated permeability

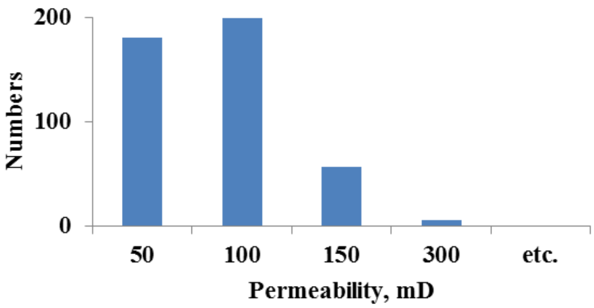

(b) Histogram of permeability

Fig. 3.29 – Updated 100 ensemble members from the random case after ES in case Ⅱ.

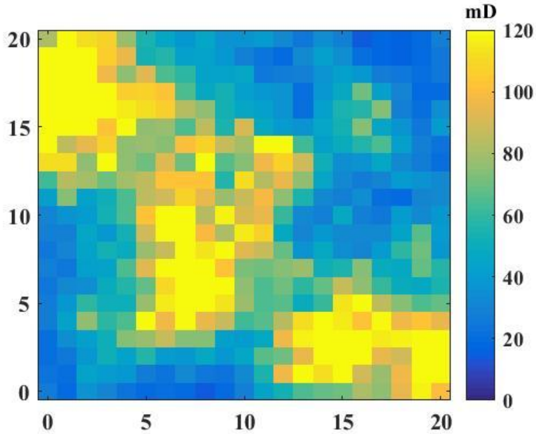

(a) The average of updated permeability

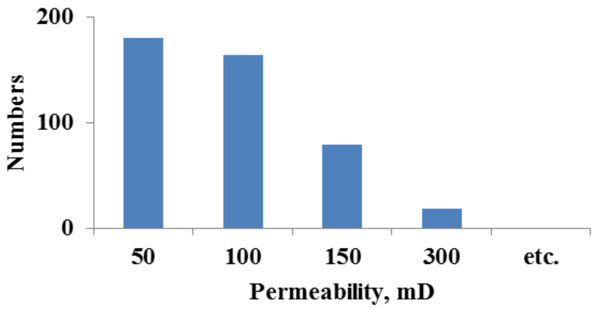

(b) Histogram of permeability

Fig. 3.30 –Updated 100 ensemble members from the 1-line case after ES in case Ⅱ.

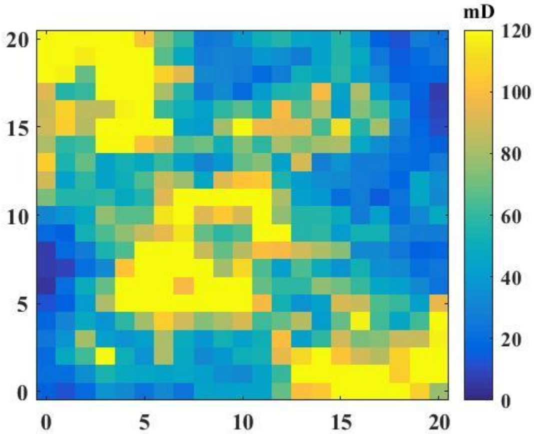

(a) The average of updated permeability

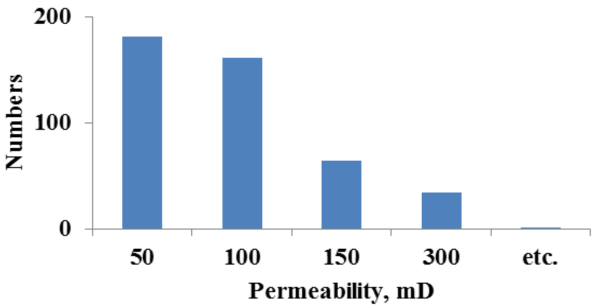

(b) Histogram of permeability

Fig. 3.31 – Updated 100 ensemble members from the cross case after ES in case Ⅱ.

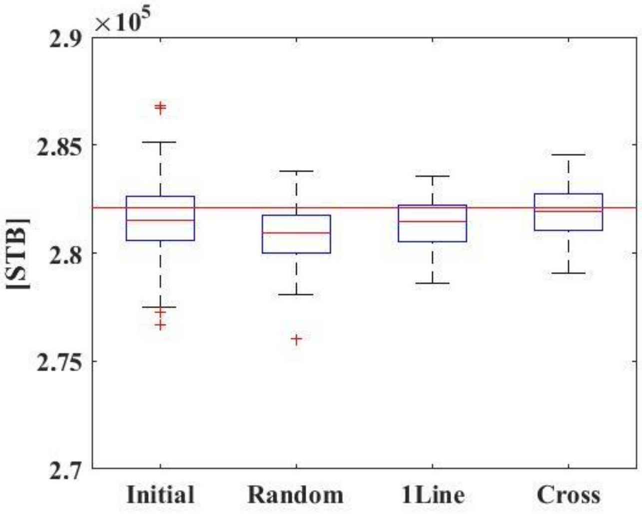

(a) Oil

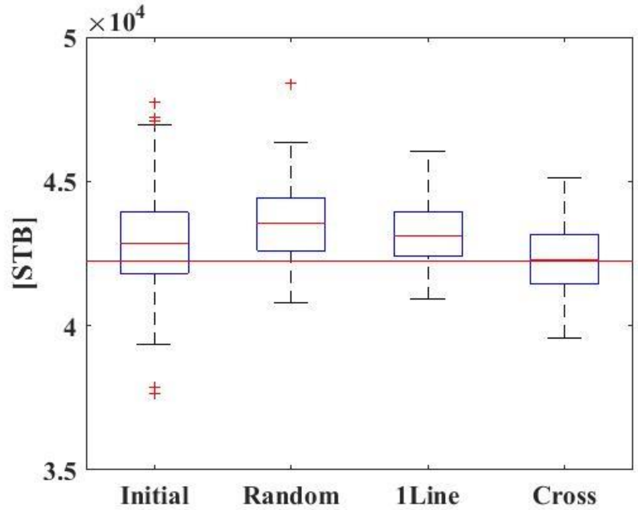

(b) Water

Fig. 3.32 –Box plots for cumulative oil and water productions from the 400 ensemble, random, 1-line, and cross cases after ES in case Ⅱ.

Table 3.3 – Total simulation time and its reduction for case Ⅱ.

	Initial	Random	One-line	Cross
Time, min	90	22	22	22
Reduced time, %	-	75	75	75

4. Conclusions

Even though many distances are suggested for sampling reservoir models, there are inefficiencies such as long calculation time or data distortion. Therefore, a new distance is proposed from the spatial pattern, which suitably considers permeability distribution of a reservoir.

There are two spatial patterns, called 1-line and cross cases, considering nine spot well locations. In this paper, the sampling effects from them are compared before and after ES application. The cross case gives the most improved results in two different field cases. The proposed method has the following advantages.

1. This study suggests a simple and fast sampling scheme for good model selection. By applying the method, high uncertainty of initial models can be reduced. Also, approximate permeability distribution of the reference field is found out.

2. The proposed distance using spatial pattern contributes to reinforce ES. With the distance-based ES method,

more precise reservoir characterization can be achieved with only 10–30% simulation time of the typical ES.

3. The cross case is helpful for good model selection with around 50 to 100 ensemble members. Also, if over 100 ensemble members are available, the cross case will produce stable ES results.

4. In comparison with the 1–line case, the cross case gives more reliable results. It shows the importance of near–well permeability data progressed from the injector to all producers when people define spatial pattern. That is because the water flowing from the injector pushes oil to producers, and affects reservoir behaviors significantly.

5. The proposed method can be a practical guideline when we try to estimate reservoir permeability distributions using limited data.

The proposed distance–based ensemble smoother can provide reliable basis on decision making, which is important in oil production. Also, this method can be used to minimize problems in well development and operation by prediction of reservoir behavior in the future.

Although this method is simple and fast for good reservoir model selection, it can be only a guideline to define proper spatial pattern. For a further study, it is important to define spatial pattern which reflects permeability characteristics of each field type. We find out flow pattern of reference field approximately. Therefore, we can decide spatial pattern which considers the flow pattern.

References

Dubuisson M. & Jain A., 1994. A modified Hausdorff distance for object matching. Paper presented at the 12th International Conference on Pattern Recognition, Jerusalem, Israel, October 9-13. pp. 3.

Evensen G., 1994. Sequential data assimilation with a nonlinear quasi-geostrophic model using Monte Carlo methods to forecast error statistics. Journal of Geophysical Research **99**(C5), 10143-10162.

Evensen G., Hove J., Meisingset H.C., Reiso E., Seim K.S. & Espelid O., 2007. Using the EnKF for assisted history matching of a North Sea reservoir model. Paper SPE 106184 presented at the SPE Reservoir Simulation Symposium, Houston, Texas, USA, February 26-28. pp. 13.

Gervais V., Le Ravalec M., Heidari L. & Schaaf T., 2012. History-matching with ensemble-based methods: application to an underground gas storage site. Paper SPE 154475 presented at the SPE Europec/EAGE Annual Conference, Copenhagen, Denmark, June 4-7, pp. 9.

Jin J., Lim J., Lee H. & Choe J., 2011. Metric space mapping of oil sands reservoirs using streamline simulation. Geosystems Engineering **14**(3), 79-84.

Jung S. & Choe J., 2012. Reservoir characterization using a streamline-assisted ensemble Kalman filter with covariance localization. Energy Exploration & Exploitation **30**(4), 645-660.

Kang B., Lee K. & Choe J., 2016. Improvement of ensemble smoother with SVD-assisted sampling scheme. Journal of Petroleum Science and Engineering **141**, 114-124.

Lee K., Jeong H., Jung S. & Choe J., 2013. Characterization of channelized reservoir using ensemble Kalman filter with clustered covariance. Energy Exploration & Exploitation **31**(1), 17-29.

Lee K., Jeong H., Jung S. & Choe J., 2013. Improvement of ensemble smoother with clustered covariance for channelized reservoirs. Energy Exploration & Exploitation **31**(5), 713-726.

Lee H., Jin J., Shin H. & Choe J., 2015. Efficient prediction of SAGD productions using static factor clustering. ASME Journal of Energy Resources Technology **137**(3), 32907-32913.

Nævdal G., Mannseth T., & Vefring E.H., 2002. Near-well reservoir monitoring through ensemble Kalman filter. Paper SPE 75235 presented at the SPE/DOE Improved Oil Recovery Symposium, Oklahoma, Texas, USA, April 13-17. pp. 9.

Park J., Jin J. & Choe J., 2015. Uncertainty quantification using streamline based inversion and distance based clustering. ASME Journal of Energy Resources Technology **138**(1), 12906-12912.

Scheidt C. & Caers J., 2009a. Representing spatial uncertainty using distances and kernels. Mathematical Geosciences **41**(4), 387-419.

Scheidt C. & Caers J., 2009b. Uncertainty quantification in reservoir performance using distances and kernel methods-application to a West Africa deepwater turbidite reservoir. SPE Journal **14**(4), 680-692.

Shin Y., Jeong H. & Choe J., 2010. Reservoir characterization using an EnKF and anon-parametric approach for highly non-Gaussian permeability fields. Energy Sources, Part A **32**(16), 1569-1578.

Skjervheim J.A., Evensen G., Hove J., & Vabo J. G., 2011. An Ensemble smoother for assisted history matching. Paper SPE 141929 presented at the SPE Reservoir Simulation Symposium, The Woodlands, Texas, USA, February 21-23. pp. 15.

Suzuki S. & Caers J., 2008. A distance-based prior model parameterization for constraining solutions of spatial inverse problems. Mathematical Geosciences **40**(4), 445-469.

Wen X.H. & Chen W.H., 2007. Some practical issues on real-time reservoir model updating using ensemble Kalman filter. SPE Journal **12**(2), 156-166.

국문초록

유체투과율 분포패턴에 거리기반의 앙상블 스무더를 이용한 저류층 특성화

이지윤

에너지시스템공학부

서울대학교

효과적인 저류층모델 샘플링을 위하여 두 모델 사이의 차이인 거리의 정의는 중요하다. 본 논문에서는 주입정과 생산정 사이의 공간적 유체투과율 분포의 상관계수차이를 새로운 거리로 제안하였다.

먼저, 초기 400개 모델에 제안된 거리를 계산하고 다차원척도법을 이용하여 이들을 2차원 평면에 나타낸다. 또한 K-메도이드 클러스터링을 통해 이들을 10개 그룹으로 나눈다. 각 그룹의 중심인 메도이드로부터 나온 생산량을 참조필드의 생산량과 비교하여 가장 그 차이가 가장 작은 메도이드를 대표모델로 선정한다. 대표모델 주변 총 100개 저류층모델을 선택하여 앙상블 스무더에 적용한다.

그 결과, 본 연구방법은 약 75% 감소된 시간 내 향상된 저류층 특성화 및 히스토리 매칭을 보였다. 또한 적절한 모델 샘플링으로 미래 생산량 예측 시 그 불확실성 폭이 크게 감소하였다. 본 연구는 실제 필드 내 유체투과율 파악에 도움을 줄 수 있다.

주요어: 거리기반, 앙상블 스무더, 불확실성 평가
학번: 2014-22728